Chapter 9
Caveats for Robustness

9.1 Introduction

In this chapter we consider the position-based formation control design in (2.74) and investigate its robustness with respect to switching topology, link gain variation and unmodeled dynamics. For convenience, we rewrite (2.74) here

$$(M \otimes I_p)\ddot{\mathbf{x}} + (K \otimes I_p)\dot{\mathbf{x}} + (L_\Delta \otimes I_p)\mathbf{x} = 0 \tag{9.1}$$

where $M = \text{diag}\{m_1, \cdots, m_N\}$, $K = \text{diag}\{k_1, \cdots, k_N\}$ and $L_\Delta = D\Delta D^T$ is the weighted Laplacian. Recall that (9.1) ensures global asymptotic stability of the origin of $\dot{\mathbf{x}}$ and $\mathbf{z} = (D^T \otimes I_p)\mathbf{x}$.

We first analyze (9.1) with switching topologies. Such switching may occur due to the vehicles joining or leaving a formation, transmitter/receiver failures, limited communication/sensor range, or physical obstacles temporarily blocking sensing between vehicles. For single integrator dynamics, switching topology has been studied in [63, 103] and stability under arbitrary switching has been ascertained for classes of coordination algorithms. In contrast, for second order dynamics, we illustrate with an example that a destabilizing switching sequence that triggers instability exists. We then show that stability is maintained when switching is sufficiently fast or slow so that is does not interfere with the natural frequencies of the group dynamics.

We next investigate stability properties when the link weights are perturbed by small sinusoidal oscillations. To illustrate this instability in its most basic form, we make a simplifying assumption that the perturbation is sinusoidal and transform the group dynamics into a form that reveals a parametric resonance mechanism [52, 96, 53]. This transformation employs the spectral properties of the graph Laplacian and decouples the relative motion from the motion of the center of the agents. When mass inertia and damping terms are identical for all agents, we obtain decoupled *Mathieu equations* [96], which make parametric resonance explicit. For broader classes of mass and damping matrices, we obtain coupled Mathieu equations and discuss which frequencies lead to parametric resonance. Next, we show

H. Bai et al., *Cooperative Control Design: A Systematic, Passivity-Based Approach*, Communications and Control Engineering 89, DOI 10.1007/978-1-4614-0014-1_9,

that sinusoidal perturbations do not destabilize the system if they are slow or fast enough. The sinusoidal perturbations studied in this situation are not necessarily the most commonly occurring ones in practice. However, they allow us to study worst-case scenarios to deepen the understanding of fundamental stability and robustness properties in cooperative systems.

We finally study the effect of input unmodeled dynamics, such as fast actuator dynamics. Following standard singular perturbation arguments, we prove that the stability of the nominal design that ignores the effects of unmodeled dynamics is preserved when the stable unmodeled dynamics are sufficiently fast. As we illustrate with an example, how fast the unmodeled dynamics must be is dictated by the graph structure and the mass inertia matrix.

9.2 Instability due to Switching Topology

9.2.1 Example

Consider four agents with an undirected graph that switches between a ring graph and a complete graph[1]. Let $M = I$, $K = kI$ and $\Delta = \delta I$ for some constants $k > 0$ and $\delta > 0$. Then, the closed-loop dynamics (9.1) become

$$\ddot{\mathbf{x}} + k\dot{\mathbf{x}} + \delta(L_i \otimes I_p)\mathbf{x} = 0 \quad i = 1,2 \tag{9.2}$$

where $L_i = D_i D_i^T$ is the Laplacian matrix for the ring graph when $i = 1$, and for the complete graph when $i = 2$.

Because L_1 and L_2 admit the same set of orthonormal eigenvectors q_j, $j = 1,\cdots,4$ for their eigenvalues $\{0,2,2,4\}$ and $\{0,4,4,4\}$, respectively, the change of variables $d_j = (q_j^T \otimes I_p)\mathbf{x}$, $j = 1,\cdots,4$ decouples the dynamics (9.2) into

$$\ddot{d_j} + k\dot{d_j} + \delta\lambda_{j_i} d_j = 0, \tag{9.3}$$

where λ_{j_i} is the jth eigenvalue of the Laplacian L_i, $i = 1,2$. It then follows from standard results in switching systems [81, 1, 80] that, if the damping k is small, and if $\delta\lambda_{j_1} < 1$ and $\delta\lambda_{j_2} > 1$, then (9.3) is destabilized by a switching sequence that selects $i = 1$ when $d_j^T \dot{d}_j > 0$ and $i = 2$ otherwise. Instability with this sequence follows from the Lyapunov-like function $V = \|d_j\|^2 + \|\dot{d}_j\|^2$ which increases along the trajectories of (9.3). Because the eigenvalues λ_{2_i} and λ_{3_i} switch between the values 2 and 4 in our example, if $\delta \in (1/4, 1/2)$, then $\delta\lambda_{j_1} < 1$ and $\delta\lambda_{j_2} > 1$ indeed hold for $j = 2,3$. This means that, when the damping is small, a destabilizing switching sequence exists.

We demonstrate this instability with a simulation in Fig. 9.1. We choose $p = 1$ and four agents. Although the system (9.1) guarantees agreement of $\mathbf{x}_i$'s for any

[1] A complete graph is a graph where every two nodes are connected.

fixed connected graph, when the communication topology switches between a complete graph and a ring graph according to the sequence described above, Fig. 9.1 shows that the relative distances between the agents diverge.

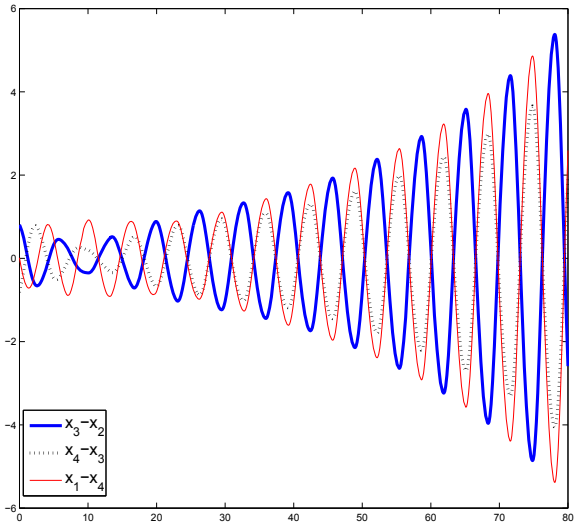

Fig. 9.1 A switching sequence described in Section 9.2.1 between the ring and complete graphs destabilizes the relative positions between the agents in the system (9.1).

9.2.2 Comparison with First-order Agent Models

The instability example presented in the previous section occurs only when the agent dynamics are second or higher order. In this section, we show that for agents modeled as first order integrators, switching between connected graphs will not lead to instability. In fact, the agreement of $\mathbf{x}_i$'s can be achieved even if the graph loses connectivity pointwise in time. Note that for first order agents, the $\mathscr{H}_i$'s in Fig. 2.2 are simply static passive blocks. We then restrict our attention to the following class of first order agreement protocols

$$\dot{\mathbf{x}}_i = -\sum_{k=1}^{M} d_{ik}(t)\,\psi_k(\mathbf{z}_k) \quad \mathbf{z}_k := \sum_{j=1}^{N} d_{jk}(t)\mathbf{x}_j, \tag{9.4}$$

rewritten in vector form (2.3), (2.24) as

$$\dot{\mathbf{x}} = -(D(t) \otimes I_p)\, \psi(\mathbf{z}) \tag{9.5}$$
$$\mathbf{z} = (D(t)^T \otimes I_p)\mathbf{x} \tag{9.6}$$

where the multivariable nonlinearity $\psi(\cdot)$ has the property (2.46). The matrix $D(t)$ is piecewise continuous because its entries exhibit step changes when a change occurs in the communication topology. We define the time varying graph Laplacian as

$$L(t) = D(t)D(t)^T. \tag{9.7}$$

If the graph remains connected for all $t \geq 0$, that is, if

$$\lambda_2\{L(t)\} \geq \sigma_c > 0 \quad \forall t \geq 0 \tag{9.8}$$

for some constant $\sigma_c > 0$ that does not depend on time, then it is not difficult to show that $\mathbf{x}_i$'s in (9.5)-(9.6) reach an agreement despite the time-varying $L(t)$. We now prove agreement under a less restrictive *persistency of excitation* condition which stipulates that graph connectivity be established over a period of time, rather than pointwise in time:

Proposition 9.1. *Consider the system (9.5)-(9.6) where $\mathbf{x} \in \mathbb{R}^{pN}$ comprises of the components $\mathbf{x}_i \in \mathbb{R}^p$, $i = 1, \cdots, N$ concatenated as in (2.3), $\psi(\cdot)$ satisfies (2.46), and $D(t)$ is piecewise continuous incidence matrix. Let S be an $(N-1) \times N$ matrix with orthonormal rows that are each orthogonal to 1_N; that is,*

$$S1_N = 0 \quad SS^T = I_{N-1}. \tag{9.9}$$

If there exist constants $\delta > 0$ and $\alpha > 0$ such that, for all $t_0 \geq 0$,

$$\int_{t_0}^{t_0+\delta} SL(t)S^T dt \geq \alpha I, \tag{9.10}$$

where $L(t)$ is defined in (9.7), then the protocol (9.5)-(9.6) achieves the agreement of $\mathbf{x}_i$'s. □

The proof of this proposition can be found in Appendix A.8. The "persistency of excitation" condition (9.10) means that $SL(t)S^T$ is nonsingular when integrated over a period of time, and not necessarily pointwise in time. Since, by construction of S in (9.9), $SL(t)S^T$ inherits all eigenvalues of $L(t)$ except the one at zero, its smallest eigenvalue is

$$\lambda_1\{SL(t)S^T\} = \lambda_2\{L(t)\}, \tag{9.11}$$

which means that nonsingularity of the matrix $SL(t)S^T$ is equivalent to connectivity of the graph. Because Proposition 9.1 does not require nonsingularity of $SL(t)S^T$ pointwise in time, it allows the graph to lose pointwise connectivity as long as it is established in the integral sense of (9.10). The pointwise connectivity situation (9.8) is a special case of Proposition 9.1 because, then, (9.10) readily holds with $\alpha = \sigma_c \delta$.

9.2.3 When is Stability Maintained?

Having demonstrated stability robustness of first order agreement protocol with respect to switching topology, we now come back to the second order protocol (9.1) and consider under what conditions the stability of (9.1) is maintained.

Since (9.1) guarantees the origin of $(\dot{\mathbf{x}}, \mathbf{z})$ to be exponentially stable for a fixed connected graph, using the concept of dwell-time [81, 91, 56], we can ensure $\dot{\mathbf{x}} \to 0$ and $\mathbf{z} \to 0$ if all graphs in the switching sequence are connected and if the interval between consecutive switchings is no shorter than some minimum dwell time $\tau > 0$, where estimates for τ can be obtained following [56]. We next employ the concept of an "average graph" to show that fast and periodic switching also preserves stability.

Consider a periodic switching sequence $\sigma(t)$ in which the topology switches $n-1$ times, $n \geq 1$, during one period T. We label n graph Laplacians in T as L_Δ^i, $i = 1, \cdots, n$ and denote their dwell times by τ_i, $i = 1, \cdots, n$, $\sum_{i=1}^n \tau_i = T$. We thus study the switched system:

$$(M \otimes I_p)\ddot{\mathbf{x}} + (K \otimes I_p)\dot{\mathbf{x}} + (L_\Delta^{\sigma(t)} \otimes I_p)\mathbf{x} = 0 \tag{9.12}$$

where

$$L_\Delta^{\sigma(t)} \in \{L_\Delta^1, L_\Delta^2, \cdots, L_\Delta^n\}. \tag{9.13}$$

To determine the stability of (9.12)-(9.13), we investigate the eigenvalues of the state transition matrix evaluated over a period T:

$$\Xi(T,0) = e^{A_N \tau_N} \cdots e^{A_2 \tau_2} e^{A_1 \tau_1}, \tag{9.14}$$

where

$$A_i = \begin{pmatrix} \mathbf{0}_N & I_N \\ -M^{-1}L_\Delta^i & -M^{-1}K \end{pmatrix} \otimes I_p \tag{9.15}$$

is the system matrix of (9.12) in the coordinates of $(\mathbf{x}, \dot{\mathbf{x}})$, $i = 1, \cdots, N$. When τ_i's are small, we rewrite (9.14) as

$$\begin{aligned} \Xi(T,0) &= \prod_{i=1}^n [I + \tau_i A_i + O(\tau_i^2)] \\ &= I + \sum_{i=1}^N \tau_i A_i + O(T^2) \\ &= I + TA^{av} + O(T^2) \end{aligned} \tag{9.16}$$

where

$$A^{av} = \begin{pmatrix} \mathbf{0}_N & I_N \\ -M^{-1}L_\Delta^{av} & -M^{-1}K \end{pmatrix} \otimes I_p \tag{9.17}$$

and

$$L_\Delta^{av} = \frac{1}{T} \sum_{i=1}^n \tau_i L_\Delta^i \tag{9.18}$$

is the average of the n graph Laplacians during the period T.

Because the linear combination (9.18) preserves the structure of a Laplacian, L_Δ^{av} defines an average graph obtained by superimposing the individual graphs $i = 1, \cdots, n$. In this average graph, the links are weighted by τ_i/T, which represents the relative dwell time of each graph constituting the average. This means that, if the time-varying graph is *jointly connected* as in [63], then the averaged graph described by L_Δ^{av} is connected. We point out that the connectedness of L_Δ^{av} also satisfies the persistency of excitation condition in (9.10) with $\delta = T$ since for all $t_0 \geq 0$

$$\int_{t_0}^{t_0+T} S L_\Delta^{\sigma(t)} S^T dt = S L_\Delta^{av} S^T, \tag{9.19}$$

which is positive definite if and only if the average graph is connected.

We finally show that, when T is sufficient small, connectedness of the average graph implies stability of (9.12)-(9.13). To see this, note from (9.16) that the eigenvalues of $\Xi(T,0)$ are given by

$$\kappa_i = 1 + T\lambda_i + O(T^2), \quad i = 1, \cdots, 2N, \tag{9.20}$$

where λ_i's are the eigenvalues of A^{av}. It follows that if the graph induced by the averaged Laplacian L_Δ^{av} is connected, then all λ_i's have negative real parts, except the one, say λ_1, at zero. This zero eigenvalue results from the null space of A^{av}, spanned by $a = [1_N^T \quad 0_N^T]^T$, which is also the null space of A_i, $i = 1, \cdots, n$. We thus conclude that $\Xi(T,0)a = a$, which implies $\kappa_1 = 1$. Then, for sufficiently small T, κ_i in (9.20), $i = 2, \cdots, 2N$, remain inside the unit circle and $\kappa_1 = 1$ corresponds to the motion of the center, thereby guaranteeing the asymptotic stability of the subspace spanned by $a = [1_N^T \quad 0_N^T]^T$. Note that convergence to this subspace guarantees $\dot{\mathbf{x}} \to 0$ and $\mathbf{z} \to 0$.

Lemma 9.1. *Consider the closed loop dynamics (9.12)-(9.13) with a switching signal $\sigma(t)$ of period T. If the averaged graph induced by (9.18) is connected, then there exists a T^*, such that for $T < T^*$, the the subspace spanned by $a = [1_N^T \quad 0_N^T]^T$ is asymptotically stable.* □

9.3 Parametric Resonance

9.3.1 Example

To illustrate parametric resonance in its most basic form, we study an example of the cooperative system (9.1) with $M = I$, $K = kI$ and $\Delta = \delta I$. To further simplify the notation we consider the single degree-of-freedom case $p = 1$. The same analysis extends to $p > 1$ with the use of Kronecker algebra. The graph is now time-invariant but the link gain δ is perturbed by a cosine term $\varepsilon \cos \omega t$, thus leading to the closed-loop model

$$\ddot{\mathbf{x}} + k\dot{\mathbf{x}} + (\delta + \varepsilon \cos \omega t) L\mathbf{x} = 0. \tag{9.21}$$

Note from Property 1.2 that L can be diagonalized by an orthonormal matrix Q:

$$Q^T LQ = L_d := \text{diag}\{\lambda_N, \cdots, \lambda_1\} \tag{9.22}$$

where $\lambda_N \geq \lambda_{N-1} \geq \cdots \geq \lambda_1 = 0$. If follows from Property 1.3 that if the graph is connected, then only λ_1 is zero and the corresponding column in Q is $\frac{1}{\sqrt{N}} 1_N$ due to Property 1.1. Thus, we let

$$Q = [S^T \frac{1}{\sqrt{N}} 1_N] \tag{9.23}$$

where S satisfies (9.9), and decompose $\mathbf{x}$ as

$$\mathbf{x} = S^T d + \frac{1_N}{\sqrt{N}} c, \tag{9.24}$$

where $d \in \mathbb{R}^{N-1}$ and $c \in \mathbb{R}$.

The dynamics of c correspond to the evolution of the center of $\mathbf{x}$ and is obtained by premultiplying (9.21) by $\frac{1}{\sqrt{N}} 1_N^T$:

$$\ddot{c} + k\dot{c} = 0. \tag{9.25}$$

The solution $c(t)$ approaches $\dot{c}(0)/k + c(0)$, which means that the time-varying link gains do not affect the motion of the center.

Next we derive the dynamic equations for d. Since $SS^T = I_{N-1}$, we obtain from (9.24) that

$$d = S\mathbf{x} \tag{9.26}$$

which, from (9.21), results in

$$\ddot{d} + k\dot{d} + (\delta + \varepsilon \cos \omega t) SL\mathbf{x} = 0. \tag{9.27}$$

We further note from (9.24) that

$$SL\mathbf{x} = SLS^T d \tag{9.28}$$

and from (9.22)-(9.23) that

$$SLS^T = \bar{L}_d \tag{9.29}$$

where $\bar{L}_d = \text{diag}\{\lambda_N, \cdots, \lambda_2\}$. Substituting (9.28)-(9.29) into (9.27), we obtain

$$\ddot{d}_j + k\dot{d}_j + (\delta + \varepsilon \cos \omega t)\lambda_{n+1-j} d_j = 0, \quad j = 1, \cdots, N-1, \tag{9.30}$$

which is a Mathieu equation [52, 149, 96] with the natural frequency $\sqrt{\delta \lambda_{N+1-j}}$. It then follows from standard results for the Mathieu equation that instability occurs when the frequency of the perturbation is around $\omega = 2\sqrt{\delta \lambda_i}/r$, $r = 1, 2, 3, \cdots$, for each $i = 2, \cdots, N$. When damping k is zero, parametric resonance occurs at these

frequencies for arbitrarily small ε. For nonzero damping k, parametric resonance occurs for sufficiently large values of ε.

9.3.2 Coupled Mathieu Equations

In the previous example, the assumptions that $M = I$ and $K = kI$ played a crucial role in obtaining the decoupled Mathieu equations (9.30). We now remove this assumption and study the case where M, K and Δ in (9.1) are diagonal matrices with not necessarily identical entries. We then reveal parametric resonance with an analysis of *coupled* Mathieu equations as in [96, Section 5.4], [149, 53, 52]. When each link gain δ_i is perturbed by $\varepsilon\bar{\delta}_i \cos\omega t$, (9.1) becomes

$$M\ddot{\mathbf{x}} + K\dot{\mathbf{x}} + D(\Delta + \varepsilon\cos\omega t\bar{\Delta})D^T\mathbf{x} = 0 \tag{9.31}$$

where $\bar{\Delta} = \mathrm{diag}\{\bar{\delta}_1, \cdots, \bar{\delta}_\ell\}$. Premultiplying by the inverse of M, we obtain

$$\ddot{\mathbf{x}} + M^{-1}K\dot{\mathbf{x}} + M^{-1}L_\Delta\mathbf{x} + \varepsilon\cos\omega t M^{-1}L_{\bar{\Delta}}\mathbf{x} = 0. \tag{9.32}$$

where $L_{\bar{\Delta}} = D\bar{\Delta}D^T$. The coordinate transformation $y = \mathscr{T}^{-1}\mathbf{x}$, where $\mathscr{T}$ is composed of the eigenvectors of $M^{-1}L_\Delta$, then leads to

$$\ddot{y} + \mathscr{T}^{-1}M^{-1}K\mathscr{T}\dot{y} + \Lambda y + \varepsilon\cos\omega t\mathscr{T}^{-1}M^{-1}L_{\bar{\Delta}}\mathscr{T}y = 0, \tag{9.33}$$

in which

$$\Lambda = \mathrm{diag}\{\hat{\lambda}_N, \cdots, \hat{\lambda}_1\} \tag{9.34}$$

and $\hat{\lambda}_i$'s are the eigenvalues of $M^{-1}L_\Delta$. Because a similarity transformation brings $M^{-1}L_\Delta$ to the symmetric form $M^{-\frac{1}{2}}L_\Delta M^{-\frac{1}{2}}$, we conclude that $\hat{\lambda}_i$'s are real and nonnegative. Because $\mathscr{N}(D^T)$ is spanned by 1_N, one of the eigenvalues of $M^{-1}D\Delta D^T$, say $\hat{\lambda}_1$, is zero and the corresponding column in $\mathscr{T}$ is 1_N. Similarly to (9.23)-(9.24), we rewrite $\mathscr{T}$ as

$$\mathscr{T} = [S \quad 1_N] \tag{9.35}$$

and note that

$$\mathbf{x} = \mathscr{T}y = Sd + 1_N c \tag{9.36}$$

where $d \in \mathbb{R}^{n-1}$, and $c \in \mathbb{R}$ is the center of $\mathbf{x}$. It then follows from (9.33) and the decomposition (9.36) that

$$\ddot{y} + \mathscr{T}^{-1}M^{-1}K\mathscr{T}\dot{y} + \Lambda y + \varepsilon\cos\omega t\mathscr{T}^{-1}M^{-1}L_{\bar{\Delta}}Sd = 0, \tag{9.37}$$

since $1_N c$ lies in $\mathscr{N}(D^T)$.

When the damping term K is small, the off-diagonal entries of $\mathscr{T}^{-1}M^{-1}K\mathscr{T}$ can be neglected [30], that is,

$$\mathscr{T}^{-1}M^{-1}K\mathscr{T} \approx \mathrm{diag}\{\bar{k}_1, \cdots, \bar{k}_N\} := \bar{K} \tag{9.38}$$

where $\bar{k}_i$ is the ith diagonal entry of $\mathscr{T}^{-1}M^{-1}K\mathscr{T}$. The dynamics in (9.37) can then be written as

$$\begin{pmatrix} \ddot{d} \\ \ddot{c} \end{pmatrix} = -\bar{K}\begin{pmatrix} \dot{d} \\ \dot{c} \end{pmatrix} - \Lambda\begin{pmatrix} d \\ c \end{pmatrix} - \varepsilon\cos\omega t\begin{pmatrix} S^*M^{-1}L_{\bar{\Delta}}S & 0 \\ \zeta M^{-1}L_{\bar{\Delta}}S & 0 \end{pmatrix}\begin{pmatrix} d \\ c \end{pmatrix} \tag{9.39}$$

where $\mathscr{T}^{-1} = \begin{pmatrix} S^* \\ \zeta \end{pmatrix}$.

We note from (9.39) that the dynamics of d are decoupled from that of c and that stability of the relative motion of the agents is determined by the d-dynamics. Results for coupled Mathieu equations in [149, 96, 52] applied to (9.39) indicate that parametric resonance occurs around the frequencies

$$\omega = \frac{\sqrt{\hat{\lambda}_j} \pm \sqrt{\hat{\lambda}_k}}{r} \quad j \neq k, \quad j,k = 2,\cdots,N. \tag{9.40}$$

and

$$\omega = \frac{2\sqrt{\hat{\lambda}_j}}{r}, \quad j = 2,\cdots,N, \quad r = 1,2,3\cdots \tag{9.41}$$

For $\bar{K} \neq 0$, parametric resonance occurs at these frequencies if ε is sufficiently large. The parametric resonance resulting from (9.40) is known as *Combination Resonance* because the excitation frequency ω is a linear combination of two natural frequencies $\sqrt{\hat{\lambda}_j}$ and $\sqrt{\hat{\lambda}_k}$ [149]. When (9.41) is satisfied, the corresponding mode, d_{N-j+1}, is excited and the resulting parametric resonance is called *Subharmonic Resonance*. Such resonances are well studied in structural mechanics literature and are not further discussed here.

9.3.3 Fast Varying Perturbation

In the examples above instability occurs when the frequency of the perturbation interferes with the natural frequencies of the cooperative system. We now show that if the perturbation is fast enough (i.e., large ω), the origin of $(\dot{\mathbf{x}}, \mathbf{z})$ is asymptotically stable. In the next subsection, we investigate slow perturbations.

Defining $\tau_f = \omega t$ and denoting

$$\frac{d(\cdot)}{d\tau_f} = (\cdot)', \tag{9.42}$$

we rewrite the perturbed model in (9.32) as

$$\omega^2\mathbf{x}'' + \omega M^{-1}K\mathbf{x}' + M^{-1}(L_\Delta + \varepsilon\cos\tau_f L_{\bar{\Delta}})\mathbf{x} = 0. \tag{9.43}$$

Using the new variables $z_f = \mathbf{z}(\tau)/\omega$, and $v_f = \mathbf{x}'$, we obtain from (9.43) that

$$\begin{pmatrix} v_f' \\ z_f' \end{pmatrix} = \frac{1}{\omega} \underbrace{\begin{pmatrix} -M^{-1}K & -M^{-1}D(\Delta + \varepsilon \cos \tau_f \bar{\Delta}) \\ D^T & \mathbf{0}_\ell \end{pmatrix}}_{A^f(\tau_f)} \begin{pmatrix} v_f \\ z_f \end{pmatrix}. \tag{9.44}$$

When ω is sufficiently large, the averaging method [69] is applicable to (9.44) and the average of $A^f(\tau_f)$ is given by

$$A^f_{av} = \frac{1}{2\pi} \int_0^{2\pi} A^f(t) dt \tag{9.45}$$

$$= \begin{pmatrix} -M^{-1}K & -M^{-1}D\Delta \\ D^T & \mathbf{0}_\ell \end{pmatrix}, \tag{9.46}$$

which is the system matrix of (9.1) written in the coordinate of $(\dot{\mathbf{x}}, \mathbf{z})$. Therefore, A^f_{av} is asymptotically stable. The following lemma is thus a consequence of Theorem B.9 in Appendix B.9:

Lemma 9.2. *Consider the closed-loop system (9.31). There exists a $\omega_f > 0$ such that for $\omega > \omega_f$, the origin of $(\dot{\mathbf{x}}, \mathbf{z})$ is asymptotically stable.* □

9.3.4 Slowly Varying Perturbation

To analyze the system (9.32) with slowly varying perturbation (small ω), we look at its system matrix $A_s(t)$ in the $(\dot{\mathbf{x}}, \mathbf{z})$-coordinates:

$$A_s(t) = \begin{pmatrix} -M^{-1}K & -M^{-1}D(\Delta + \varepsilon \cos \omega t \bar{\Delta}) \\ D^T & \mathbf{0}_\ell \end{pmatrix}. \tag{9.47}$$

Note that $(\dot{\mathbf{x}}, \mathbf{z})$ is restricted to the following subspace

$$S_x = \{(\dot{\mathbf{x}}, \mathbf{z}) | \dot{\mathbf{x}} \in \mathbb{R}^{Np}, \mathbf{z} \in \mathscr{R}(D^T \otimes I_p)\}. \tag{9.48}$$

For any fixed t, if $\Delta + \varepsilon \cos \omega t \bar{\Delta} > \mathbf{0}_\ell$, that is

$$0 \le \varepsilon < \min_{i=1,\cdots,\ell} \frac{\delta_i}{\bar{\delta}_i}, \tag{9.49}$$

it follows that the origin of $(\dot{\mathbf{x}}, \mathbf{z})$ is asymptotically stable on S_x, which implies that $A_s(t)$ restricted to S_x is Hurwitz.

We next evaluate the derivative of $A_s(t)$ as

$$\dot{A}_s(t) = \begin{pmatrix} \mathbf{0}_N & \varepsilon \omega \sin \omega t M^{-1} D \bar{\Delta} \\ \mathbf{0}_{\ell \times N} & \mathbf{0}_\ell \end{pmatrix} \tag{9.50}$$

and compute its norm:

$$\|\dot{A}_s\| = \varepsilon\omega|\sin(\omega t)|\sqrt{\lambda_{\max}\begin{pmatrix}\mathbf{0}_N & \mathbf{0}_{N\times\ell}\\ \mathbf{0}_{\ell\times N} & \Delta D^T M^{-2} D\Delta\end{pmatrix}} \tag{9.51}$$

$$= \varepsilon\omega|\sin(\omega t)|\sqrt{\lambda_{\max}(\Delta D^T M^{-2} D\Delta)} \tag{9.52}$$

$$\leq \varepsilon\omega\sqrt{\lambda_{\max}(\Delta D^T M^{-2} D\Delta)}. \tag{9.53}$$

Since $\|\dot{A}\|$ is bounded, we conclude from Theorem B.10 in Appendix B.10 that for sufficiently small ω or ε, the origin of $(\dot{\mathbf{x}}, \mathbf{z})$ of the perturbed system (9.32) is asymptotically stable.

Lemma 9.3. *Consider the closed-loop system (9.31). There exists a $\bar{\mu} > 0$ such that for $\varepsilon\omega < \bar{\mu}$, the origin of $(\dot{\mathbf{x}}, \mathbf{z})$ is asymptotically stable.* □

9.4 Unmodeled Dynamics

We consider the following closed-loop system with unmodeled dynamics, $i = 1, \cdots, N$,

$$m_i\ddot{\mathbf{x}}_i = C_i\xi_i \tag{9.54}$$

$$\varepsilon\dot{\xi}_i = A_i\xi_i + B_i\tau_i \tag{9.55}$$

where (9.55) represents the unmodeled dynamics, $\varepsilon > 0$, A_i is Hurwitz, and τ_i is defined as

$$\tau_i = -k_i\dot{\mathbf{x}}_i - \sum_{j=1}^{\ell} d_{ij}\delta_j\mathbf{z}_j. \tag{9.56}$$

When ε is small, the unmodeled dynamics are fast. We further assume that the dc gain of the unmodeled dynamics is $C_iA_i^{-1}B_i = -I$ so that the reduced model obtained by setting $\varepsilon = 0$ in (9.54)-(9.55) is identical to (9.1). It then follows from standard singular perturbation arguments (see [69, Example 11.14] reviewed in Appendix B.11) that there exists ε^* such that for $\varepsilon < \varepsilon^*$, the origin of $(\dot{\mathbf{x}}, \mathbf{z})$ is asymptotically stable.

To illustrate the dependence of ε^* on the graph and the mass inertia, we simplify the model in (9.54)-(9.55) by assuming $M^{-1}K = kI_p$, $\Delta = \delta I_\ell$, $A = -I_p$, $B = I_p$ and $C = I_p$:

$$m_i\ddot{\mathbf{x}}_i = \xi_i \tag{9.57}$$

$$\varepsilon\dot{\xi}_i = -\xi_i + \tau_i. \tag{9.58}$$

Denoting $\bar{\xi} = (M^{-1} \otimes I_p)\xi$, we rewrite (9.57)-(9.58) in the compact form:

$$\begin{pmatrix} \dot{\mathbf{x}} \\ \ddot{\mathbf{x}} \\ \dot{\xi} \end{pmatrix} = \left(\underbrace{\begin{pmatrix} \mathbf{0}_N & I_N & \mathbf{0}_N \\ \mathbf{0}_N & \mathbf{0}_N & I_N \\ -\frac{\delta}{\varepsilon}(M^{-1}L) & -\frac{k}{\varepsilon}I_N & -\frac{1}{\varepsilon}I_N \end{pmatrix}}_{A} \otimes I_p \right) \begin{pmatrix} \mathbf{x} \\ \dot{\mathbf{x}} \\ \bar{\xi} \end{pmatrix}. \tag{9.59}$$

Then, it is not difficult to show that the $3N$ eigenvalues of A are the roots of the following N characteristic polynomials:

$$s^3 + \frac{1}{\varepsilon}s^2 + \frac{k}{\varepsilon}s + \frac{\delta}{\varepsilon}\bar{\lambda}_i = 0, \quad i = 1, \cdots, N, \tag{9.60}$$

where $\bar{\lambda}_i$'s are the eigenvalues of $M^{-1}L$. A Routh-Hurwitz argument further shows that the exact stability region in the parameter space is given by

$$\varepsilon < \varepsilon^* = \frac{k}{\delta \bar{\lambda}_{\max}}, \tag{9.61}$$

where $\bar{\lambda}_{\max}$ is the maximal eigenvalue of $M^{-1}L$. For sufficiently small ε, (9.61) is satisfied and guarantees stability despite the unmodeled dynamics. Denoting $m_{\min} = \min_i m_i$, we note that a conservative upper bound of $\bar{\lambda}_{\max}$ is $\frac{N}{m_{\min}}$, which implies from (9.61) that if $\varepsilon < \frac{k m_{\min}}{\delta N}$, the origin of $(\dot{\mathbf{x}}, \mathbf{z})$ is stable.

Note that, since $\bar{\lambda}_{\max}$ is the maximal eigenvalue of $M^{-1}L$, ε^* depends not only on the graph structure, but also on the mass distribution of the agents. To illustrate this dependence, we consider four agents with $k = 2$, $\delta = 1$ and $p = 1$. We compare ε^*'s under two graphs as in Fig. 9.2. When $M = \text{diag}\{5, 3, 2, 1\}$, we compute from (9.61) $\varepsilon^* = 1.4797$ for the star graph and $\varepsilon^* = 0.8154$ for the string graph, which means that the star graph is more robust for this M. However, when $M = I_4$, $\varepsilon^* = 0.5, 0.5858$, respectively, for the star graph and the string graph, which implies that the star graph is now less robust.

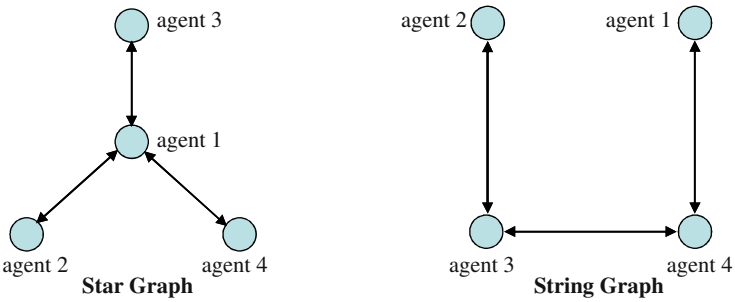

Fig. 9.2 The two graphs used in Section 9.4 to illustrate the dependence of ε^* on the graph structure and mass distribution.

9.5 Summary

In this chapter, we investigated robustness of (2.74) with respect to switching topology, link gain variation and unmodeled dynamics. We illustrated with an example that switching topology can lead to instability and showed that the closed-loop stability is maintained when switching is sufficiently fast and periodic. As a comparison, we also demonstrated that first order agreement protocols have the stability robustness with respect to switching topology. We next revealed a parametric resonance mechanism by transforming the cooperative system with time-varying link gains into Mathieu equations. As in the case of switching graphs, stability is maintained when the sinusoidal perturbation is slow or fast enough that it does not interfere with the natural frequencies of the group dynamics. We finally showed that for fast stable input unmodeled dynamics, the stability of the nominal design is preserved.

Robustness of cooperative control protocols is an area that requires further investigation. Besides the three instability mechanisms presented in this chapter, other instability mechanisms should be revealed and robust redesigns need to be developed.